

ASYMPTOTICS OF A THERMAL WAVE IN ONE-DIMENSIONAL HARMONIC CRYSTAL

A.M. Krivtsov^{1,2}, E.A. Podolskaya^{1,2*}, V.Yu. Shubina²

¹Institute for Problems in Mechanical Engineering RAS, 61, Bolshoy pr. V. O., St. Petersburg, Russia

²Peter the Great St. Petersburg Polytechnic University, 29, Politechnicheskaya str., St. Petersburg, Russia

*e-mail: katepodolskaya@gmail.com

Abstract. An asymptotic representation is obtained at large times for the thermal wavefront propagating in a one-dimensional harmonic crystal. The propagation of thermal waves from a localized thermal perturbation and the transition zone between regions with different temperatures is considered. An explicit solution is given for a number of the simplest forms of the initial temperature distribution. It is shown that during the wave evolution, the wavefront smoothes, e.g., for a power-law dependence its degree increases by 1/2.

Keywords: low-dimensional materials, discrete media, thermal processes, anomalous heat transfer, harmonic crystal, localized perturbations, asymptotics, wavefront

1. Introduction

An understanding of the heat transfer process at the micro-level is necessary to obtain the relationship between the microscopic and macroscopic descriptions of solids [1-5]. Experimental studies indicate that ballistic heat transfer dominates at the micro-level [6,7], in contrast to the macro level where diffusion heat conductivity prevails. This fact motivates interest in the simplest lattice models, in particular, in one-dimensional harmonic crystals (chains), where the anomalies associated with the ballistic nature of heat transfer are most pronounced [1,4,8-11].

In paper [12] an analytical approach for the description of the heat transfer in a one-dimensional harmonic crystal was proposed. In particular, it was shown that heat in such systems propagates in a wave manner; however, the nature of the waves is different from the waves described by the usual wave equation. Similar behavior was demonstrated for two-dimensional and polyatomic lattices using the same approach (see [13] and references therein). In [14], solutions were constructed for an equation describing the anomalous heat transfer: exact analytical solutions were obtained for a rectangular, triangular, and sawtooth initial localized perturbations, and, unlike those for the classical heat equation, they turned out to have a distinct wavefront. The examination of analytical and numerical solutions shows that the waves quickly reach a quasistationary regime, in which near the front the wave changes as follows: it decays proportionally to the square root of time, but the shape remains unchanged.

This paper focuses on the behavior of thermal waves at large times. It is shown that the waveform is described by a simple relation, which allows visual linking of the initial perturbation shape with the wave profile in the steady-state regime. This work continues the study of the evolution of localized thermal perturbations presented in [14]. The analytical relationship between the steady-state waveform and the initial perturbation profile is derived, and several illustrative examples are considered.

2. Asymptotic formulae in the case of a localized thermal perturbation

Heat transfer in a one-dimensional harmonic crystal is described by the integral formula [15]:

$$T(x, t) = \frac{1}{\pi} \int_{-\frac{\pi}{2}}^{\frac{\pi}{2}} T_0(x - ct \sin \phi) d\phi, \quad (1)$$

where T and T_0 are current and initial kinetic temperatures [4,12-15], further referred to as temperatures, c is the speed of sound in crystal, x and t are spatial coordinate and time. The kinetic temperature at a particular point x is introduced proportionally to the mean kinetic energy of the respective particle located at the same point.

Suppose that the initial perturbation is localized in space, i.e.

$$T_0(x) = \tilde{T}_0(x) \text{ for } |x| \leq l, \quad T_0(x) = 0 \text{ for } |x| \geq l, \quad (2)$$

where l is a half-width of localized perturbation, $\tilde{T}_0(x)$ represents the temperature profile in the localization zone. The solution of the equation (1) gives two thermal waves traveling in opposite directions at speed equal to c .

Consider a wave traveling in the direction of the increase of the spatial coordinate x . We introduce a new variable $z = x - ct$, which is equal to zero at the wavefront. Then, formula (1) yields to

$$T(x, t) = \frac{1}{\pi} \int_{-\frac{\pi}{2}}^{\frac{\pi}{2}} T_0(z + ct(1 - \sin \phi)) d\phi. \quad (3)$$

Assuming

$$z \sim l, \quad ct \gg l, \quad (4)$$

we further restrict ourselves to consideration of the vicinity of the wavefront at large times. Then the integrand in (3) will be nonzero only for ϕ close to $\pi/2$.

Let us introduce another variable $p^2 = ct/2l(\pi/2 - \phi)^2$ and assume that $(\pi/2 - \phi)$ is infinitesimal. Then, as a first approximation, we have

$$T(\hat{z}, t) = \frac{1}{\pi} \sqrt{\frac{2l}{ct}} \int_0^{p_{\max}} T_0(\hat{z} + p^2) dp, \quad (5)$$

where p_{\max} is the value of p , after which the integrand becomes zero, and also a dimensionless variable $\hat{z} = z/l$ is introduced.

Thus, the solution in the vicinity of the wavefront has the form

$$T(\hat{z}, t) = \sqrt{\frac{2l}{ct}} \Phi(\hat{z}), \quad (6)$$

where $\Phi(\hat{z})$ is a function that characterizes the shape of the thermal wave, from now on referred to as shape function. From (6) it follows that the wave profile shrinks vertically with time as $1/\sqrt{t}$, but it does not change horizontally, i.e., its "width" remains the same.

We specify the integration limits from the condition that the integrand function vanishes, so the final formula for the shape function becomes:

$$\begin{aligned}
 -1 \leq \hat{z} \leq 1: \quad \Phi(\hat{z}) &= \frac{1}{\pi} \int_0^{\sqrt{1-\hat{z}}} \tilde{T}_0(\hat{z} + p^2) dp, \\
 \hat{z} \leq -1: \quad \Phi(\hat{z}) &= \frac{1}{\pi} \int_{\sqrt{-1-\hat{z}}}^{\sqrt{1-\hat{z}}} \tilde{T}_0(\hat{z} + p^2) dp.
 \end{aligned}
 \tag{7}$$

Here, the general representation for the initial temperature distribution T_0 (2) is replaced by its value \tilde{T}_0 in the localization zone.

The derivative of (7) near the wavefront, i.e., for $-1 \leq \hat{z} \leq 1$, is also of interest:

$$\frac{d\Phi}{d\hat{z}} = \frac{1}{\pi} \left[\int_0^{\sqrt{1-\hat{z}}} \frac{\partial \tilde{T}_0(\hat{z} + p^2)}{\partial \hat{z}} dp - \frac{\tilde{T}_0|_{\hat{z}=1}}{2\sqrt{1-\hat{z}}} \right].
 \tag{8}$$

We see that if the initial temperature at the right boundary of the localization zone is not equal to zero, i.e. $\tilde{T}_0|_{\hat{z}=1} \neq 0$, then the derivative (8) tends to infinity at the wavefront, regardless of the particular shape of the profile. If $\tilde{T}_0|_{\hat{z}=1} = 0$ the second term vanishes, and the shape of the initial perturbation determines the slope of the tangent to the front. Similarly, differentiating the second part of the formula (7), we obtain that if $\tilde{T}_0|_{\hat{z}=-1} \neq 0$, then the derivative of (7) on the left boundary is also infinite, which leads to a break in the profile at the critical point $\hat{z} = -1$.

3. Examples of wave propagation from a localized perturbation

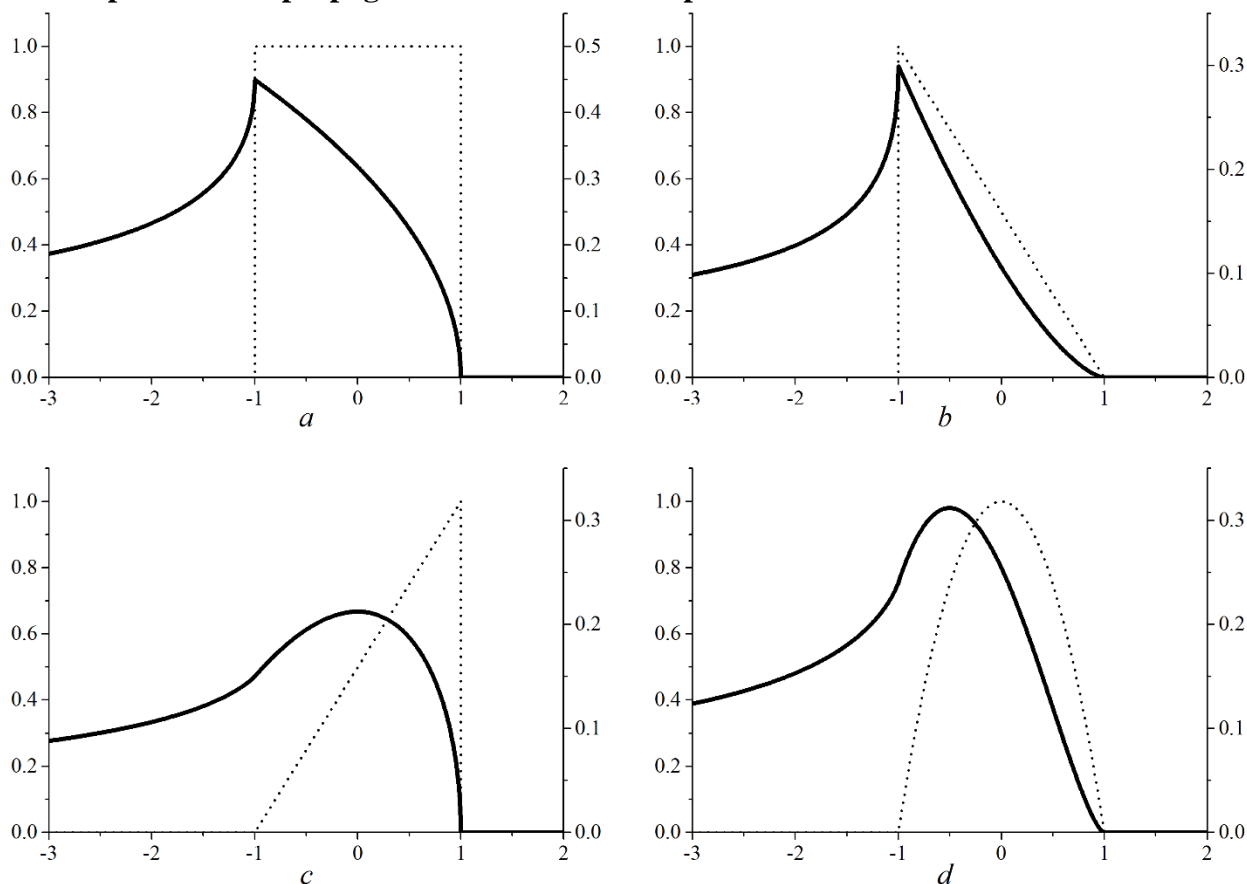


Fig. 1. Evolution of rectangular (9), sawtooth (11) and (14), and parabolic (19) profiles

Figure 1 demonstrates the temperature profiles for several examples discussed below: (a) rectangular profile, (b) and (c) sawtooth profiles, and (d) parabolic profile. The dotted line shows the initial profile $\tilde{T}_0(x)$ in the localization zone, the solid line is the shape function $\Phi(\hat{z})$. Normalization along the horizontal axis is carried out with respect to the localization radius l , along the vertical axes – to the maximum initial temperature \tilde{T}_0^{\max} . Note that the initial "dotted" profile transforms into two peaks traveling in the opposite direction, and only the right one, which moves in the direction of the increase of spatial coordinate, is displayed "solid" in Fig. 1.

Rectangular profile. Let $\tilde{T}_0 = A = \text{const}$. Then from formulae (7) and (8) we immediately obtain:

$$\begin{aligned} -1 \leq \hat{z} \leq 1: \quad \Phi &= \frac{A}{\pi} \sqrt{1 - \hat{z}}, \\ \hat{z} \leq -1: \quad \Phi &= \frac{A}{\pi} (\sqrt{1 - \hat{z}} - \sqrt{-1 - \hat{z}}), \\ \hat{z} \rightarrow \pm 1: \quad \frac{d\Phi}{d\hat{z}} &= \mp \infty. \end{aligned} \quad (9)$$

Thus, the main part of the wave is described by the root function, and the wave tail is the difference of two root functions (see Fig. 1a). A break in the temperature profile is observed, and the maximum temperature value is reached at $\hat{z} = -1$:

$$T^{\max} = \sqrt{\frac{2l}{ct}} \Phi^{\max} = \frac{2A}{\pi} \sqrt{\frac{l}{ct}}. \quad (10)$$

Sawtooth profile 1. Consider

$$\tilde{T}_0 = A \frac{l - x}{2l}. \quad (11)$$

The solution is as follows (see Fig. 1b)

$$\begin{aligned} -1 \leq \hat{z} \leq 1: \quad \Phi &= \frac{A}{3\pi} (1 - \hat{z})^{3/2}, \\ \hat{z} \leq -1: \quad \Phi &= \frac{A}{3\pi} \left[(1 - \hat{z})^{3/2} - (2 - \hat{z})\sqrt{-1 - \hat{z}} \right], \\ \hat{z} \rightarrow -1: \quad \frac{d\Phi}{d\hat{z}} &= \infty, \\ \hat{z} \rightarrow 1: \quad \frac{d\Phi}{d\hat{z}} &= 0. \end{aligned} \quad (12)$$

The maximum temperature value

$$T^{\max} = \frac{4A}{3\pi} \sqrt{\frac{l}{ct}} \quad (13)$$

is also reached at the $\hat{z} = -1$, where the derivative of the solution has a jump.

Sawtooth profile 2. Let

$$\tilde{T}_0 = A \frac{l + x}{2l} \quad (14)$$

Formula (14) is similar to (11), but the profile of the corresponding solution is significantly different (see Fig. 1c):

$$\begin{aligned}
-1 \leq \hat{z} \leq 1: \quad \Phi &= \frac{A}{3\pi} (2 + \hat{z}) \sqrt{1 - \hat{z}}, \\
\hat{z} \leq -1: \quad \Phi &= \frac{A}{3\pi} \left[(-1 - \hat{z})^{3/2} + (2 + \hat{z}) \sqrt{-1 - \hat{z}} \right], \\
\hat{z} \rightarrow -1: \quad \frac{d\Phi}{d\hat{z}} &\neq \infty, \\
\hat{z} \rightarrow 1: \quad \frac{d\Phi}{d\hat{z}} &= -\infty.
\end{aligned} \tag{15}$$

In contrast to the previous example, there is no break in profile at $\hat{z} = -1$, and the maximum temperature value is reached at $\hat{z} = 0$:

$$T^{\max} = \frac{2A}{3\pi} \sqrt{\frac{l}{ct}}. \tag{16}$$

Parabolic profile. Consider one of the simplest forms of a curvilinear profile:

$$\tilde{T}_0 = A \frac{l^2 - x^2}{l^2}. \tag{17}$$

The solution looks like (see Fig. 1d):

$$\begin{aligned}
-1 \leq \hat{z} \leq 1: \quad \Phi &= \frac{4A}{15\pi} (3 + 2\hat{z})(1 - \hat{z})^{3/2}, \\
\hat{z} \leq -1: \quad \Phi &= \frac{4A}{15\pi} \left[(3 + 2\hat{z})(1 - \hat{z})^{3/2} + (3 - 2\hat{z})(-1 - \hat{z})^{3/2} \right], \\
\hat{z} \rightarrow -1: \quad \frac{d\Phi}{d\hat{z}} &\neq \infty, \\
\hat{z} \rightarrow 1: \quad \frac{d\Phi}{d\hat{z}} &= 0.
\end{aligned} \tag{18}$$

The maximum temperature value

$$T^{\max} = \frac{4A}{5\pi} \sqrt{\frac{3l}{ct}} \tag{19}$$

is reached at $\hat{z} \leq -1/2$ and there is no break at the point, where the main wave and the wave tail merge.

4. Cold and hot half-space contact

Suppose that the initial temperature distribution consists of two semi-infinite regions with different temperatures, which do not depend on spatial coordinate, as well as a localized transition zone, characterized by a given temperature distribution. For definiteness let

$$T_0(x) = A \text{ for } x \leq -l, \quad T_0(x) = \tilde{T}_0(x) \text{ for } |x| \leq l, \quad T_0(x) = 0 \text{ for } x \geq l, \tag{20}$$

where $A > 0$ is a certain constant temperature value, l is a half-width of perturbation zone, and $\tilde{T}_0(x)$ represents the temperature profile in the localization zone.

As in the case of localized perturbation (2), two thermal waves arise, traveling in opposite directions with speed equal to c . However, in contrast to the previous case, there will be both the heating wave running in the direction of the increase of spatial coordinate x , and the cooling wave traveling in the opposite direction.

Let us consider the neighborhood of the heating wavefront at large times. Using the same methodology as above, and following formulae (3)-(5), which remain unchanged, we introduce the shape function (6) and obtain the following analog of formulae (7):

$$\begin{aligned}
 -1 \leq \hat{z} \leq 1: \quad \Phi(\hat{z}) &= \frac{1}{\pi} \int_0^{\sqrt{1-\hat{z}}} \tilde{T}_0(\hat{z} + p^2) dp, \\
 \hat{z} \leq -1: \quad \Phi(\hat{z}) &= \frac{1}{\pi} \left[\int_{\sqrt{-1-\hat{z}}}^{\sqrt{1-\hat{z}}} \tilde{T}_0(\hat{z} + p^2) dp + A\sqrt{-1-\hat{z}} \right].
 \end{aligned}
 \tag{21}$$

Formulae (7) and (21) coincide in the region $|\hat{z}| \leq 1$. For $\hat{z} \leq -1$, the difference lies in the term $A\sqrt{-1-\hat{z}}$. This term describes the increase in temperature due to the influx of heat from the hot region of the crystal that has a constant temperature $A > 0$.

The Figures demonstrate the temperature profiles for the two examples discussed below: (a) temperature jump and (b) linear temperature transition. The dotted line shows the initial profile $\tilde{T}_0(x)$ in the localization zone, the solid line is the shape function $\Phi(\hat{z})$. Normalization along the horizontal axis is carried out with respect to the localization radius l , along the vertical axes – to the maximum initial temperature \tilde{T}_0^{\max} .

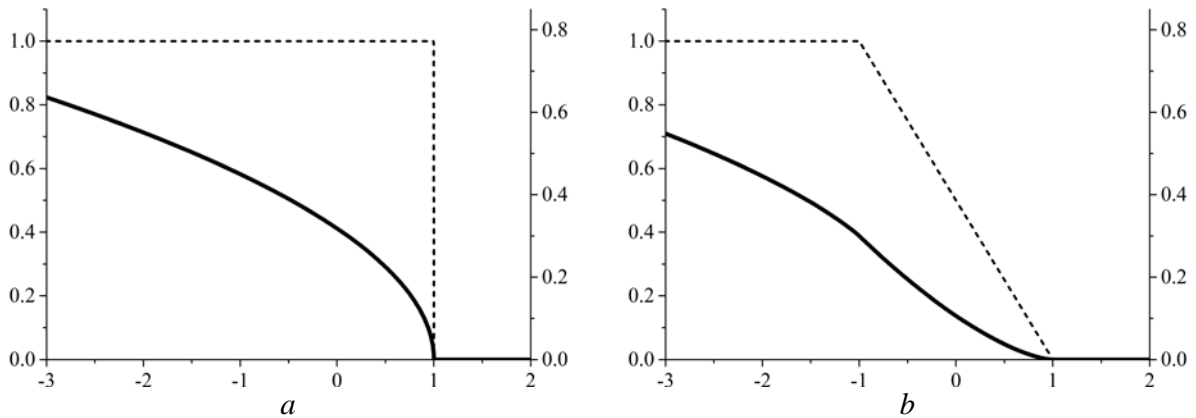


Fig. 2. Evolution of the boundaries of the temperature jump and linear temperature transition

Temperature jump. Let, $\tilde{T}_0 = A$. Then from formulae (21) we obtain that on both intervals the solution is the same and has the form:

$$\hat{z} \leq 1: \quad \Phi = \frac{A}{\pi} \sqrt{1-\hat{z}}.
 \tag{22}$$

Thus, both the main part of the wave and the tail are described by the same root function; there is no break in the temperature profile; the profile decreases monotonically with the increase of the dimensionless coordinate \hat{z} .

Linear temperature transition. Consider $\tilde{T}_0 = A^l - x/2l$, i.e., sawtooth profile (11). Then,

$$\int_0^{\sqrt{1-\hat{z}}} \tilde{T}_0(\hat{z} + p^2) dp = \frac{A}{2} \int_0^{\sqrt{1-\hat{z}}} (1 - \hat{z} - p^2) dp = \frac{A}{3} (1 - \hat{z})^{3/2}.
 \tag{23}$$

Let us now consider $\tilde{T}_0 - A = -A^l + x/2l$, i.e., sawtooth profile (14) with the opposite sign, so that

$$\int_0^{\sqrt{-1-\hat{z}}} (\tilde{T}_0(\hat{z} + p^2) - A) dp = -\frac{A}{2} \int_0^{\sqrt{-1-\hat{z}}} (1 + \hat{z} + p^2) dp = \frac{A}{3} (-1 - \hat{z})^{3/2}.
 \tag{24}$$

Finally, we obtain

$$\begin{aligned} -1 \leq \hat{z} \leq 1: \quad \Phi(\hat{z}) &= \frac{A}{3\pi} (1 - \hat{z})^{3/2}, \\ \hat{z} \leq -1: \quad \Phi(\hat{z}) &= \frac{A}{3\pi} \left[(1 - \hat{z})^{3/2} - (-1 - \hat{z})^{3/2} \right]. \end{aligned} \quad (25)$$

Unlike the previous example, where the front has a vertical tangent (which is associated with the presence of the step in the initial temperature profile), in this case the front has a horizontal tangent. In other words, the wave does not begin abruptly, and there is no jump in the derivative at the front. There is also no discontinuity of the derivative at the point $\hat{z} = -1$, at which a smooth change in the wave profile occurs. Note that a motionless observer detecting a thermal wave passing by, will notice that profile growth slows down after this point, which is associated with the appearance of the second term in formula (25).

5. On the nature of the profile at the beginning of the thermal wavefront

In this section we look into the nature of the profile at the beginning of the front of a steady thermal wave, and how it depends on the initial temperature profile. The results below are suitable for both of the above problems: when waves originate from a localized thermal perturbation and a transition zone between regions with different temperatures.

Consider formula (7) for \hat{z} close to 1. Let us denote $y = 1 - \hat{z}$, then formula (7) can be written as

$$\Phi = \frac{1}{\pi} \int_0^{\sqrt{y}} \tilde{T}_0(1 - y + p^2) dp. \quad (26)$$

We assume that the initial profile has the following character for small y :

$$\tilde{T}_0(y) \sim y^\alpha. \quad (27)$$

Then the formula (26) in the first approximation takes the form

$$\Phi(\alpha, y) = \frac{1}{\pi} \int_0^{\sqrt{y}} (y - p^2)^\alpha dp. \quad (28)$$

Calculation of the integral gives

$$\Phi(\alpha, y) = \frac{\Gamma(\alpha + 1)}{2\sqrt{\pi}\Gamma(\alpha + \frac{3}{2})} y^{\alpha + \frac{1}{2}}, \quad (29)$$

where $\Gamma(\alpha)$ is the gamma function. The shape functions $\Phi(\alpha, y)$ for several values of α are:

$$\Phi\left(-\frac{1}{2}, y\right) = \frac{1}{2}, \quad \Phi(0, y) = \frac{y}{\pi}, \quad \Phi\left(\frac{1}{2}, y\right) = \frac{y}{4}, \quad \Phi(1, y) = \frac{2y^{3/2}}{3\pi}. \quad (30)$$

Thus, as a result of the stabilization of the wave, the wavefront profile smoothes: its degree increases by $1/2$:

- if the initial profile has a singularity $1/\sqrt{y}$, then the steady front is a step;
- a step turns into a root function \sqrt{y} ;
- the root function turns to the front with linear growth;
- a linear front turns into a smooth dependence $y^{3/2}$, etc.

Since the considered problem is linear and the superposition principle is applicable, the listed properties of the transformation must be valid not only for the boundary point of the profile but also for any singular point on the initial temperature profile.

6. Conclusions

In the present work, we obtain an asymptotic representation at large times for a neighborhood of the front of a thermal wave propagating in a one-dimensional harmonic crystal (1). In contrast to the solutions for the classical heat equation, (1) has a strongly pronounced wavefront. We consider the propagation of waves from a localized thermal perturbation (2) and a transition zone between regions with different temperatures (20); explicit solutions are obtained for several simplest forms of the initial temperature perturbation.

The solution to the problem of localized thermal disturbance (7) shows that the main part of the wave is located in a space region of the same size as the initial localization zone. The thermal wave decays with time as $1/\sqrt{t}$, and the function Φ , which characterizes the shape of the profile and is proportional to T/\sqrt{t} remains unchanged. Consequently, the traveling wave shrinks vertically; however, in the horizontal direction its shape is preserved. Besides, a jump in the temperature perturbation on the left or right boundary of the localization zone at the initial time leads, respectively, to a discontinuity of the derivative at the point where the main part of the wave and the wave tail merge, or to an abrupt start of the front.

The conclusions drawn basing on formulae (7) - (8) for a localized perturbation are also preserved for the case of a transition zone between regions with different temperatures. In addition, we demonstrate that during the wave evolution, the wavefront smoothes, e.g., for a power-law dependence, its degree increases by $1/2$.

The revealed properties of the obtained solutions can be used to analyze the experimental data and to choose the correct model for the description of the heat transfer processes in low-dimensional systems.

Acknowledgments. *This work was supported by the Russian Science Foundation (project 18-11-00201, A.M. Krivtsov, project 17-71-10212, E.A. Podolskaya).*

References

- [1] Lepri S. *Thermal transport in low dimensions: from statistical physics to nanoscale heat transfer*. Springer; 2016.
- [2] Hoover W, Hoover C. *Simulation and control of chaotic nonequilibrium systems*. World Scientific; 2015.
- [3] Charlotte M., Truskinovsky L. Lattice dynamics from a continuum viewpoint. *Journal of the Mechanics and Physics of Solids*. 2012;60(8): 1508-1544.
- [4] Krivtsov A, Kuzkin V. Discrete and continuum thermomechanics. ArXiv [Preprint] 2017. Available from: <https://arxiv.org/abs/1707.09510>.
- [5] Goldstein R, Morozov N. Mechanics of deformation and fracture of nanomaterials and nanotechnology. *Physical Mesomechanics*. 2007;10(5-6): 235-246
- [6] Xu X, Pereira L, Wang Y, Wu J, Zhang K, Zhao X, Bae S, Bui C, Xie R, Thong J, Hong B, Loh K, Donadio D, Li B, Ozyilmaz B. Length dependent thermal conductivity in suspended single-layer graphene. *Nature communications*. 2014;5: 3689.
- [7] Hsiao T, Huang B, Chang H, Liou S, Chu M, Lee S, Chang C. Micron-scale ballistic thermal conduction and suppressed thermal conductivity in heterogeneously interfaced nanowires. *Physical Review B*. 2015;91(3): 035406.
- [8] Dhar A, Dandekar R. Heat transport and current fluctuations in harmonic crystals. *Physica A*. 2015;418: 49-64.
- [9] Gendelman O, Savin A. Nonstationary heat conduction in one-dimensional chains with conserved momentum. *Physical Review E*. 2010;81(2): 020103.

- [10] Guzev M. The Fourier law for a one-dimensional crystal. *Dal'nevostochnyi Matematicheskii Zhurnal*. 2018;18(1): 34-38. (In Russian)
- [11] Saadatmand D, Xiong D, Kuzkin V, Krivtsov A, Savin A, Dmitriev S. Discrete breathers assist energy transfer to ac driven nonlinear chains. *Physical Review E*. 2018;97(2): 022217.
- [12] Krivtsov A. Heat transfer in infinite harmonic one-dimensional crystals. *Doklady Physics*. 2015;60(9): 407-411.
- [13] Kuzkin V. Unsteady ballistic heat transport in harmonic crystals with polyatomic unit cell. *Continuum Mechanics and Thermodynamics*. 2019;31(6):1573-1599.
- [14] Sokolov A, Krivtsov A, Müller W. Localized heat perturbation in harmonic 1D crystals: Solutions for the equation of anomalous heat conduction. *Physical Mesomechanics*. 2017;20(3): 305-310.
- [15] Krivtsov A. The Ballistic Heat Equation for a One-Dimensional Harmonic Crystal. In: Altenbach H, Belyaev A, Eremeyev V, Krivtsov A, Porubov A. (eds.) *Dynamical Processes in Generalized Continua and Structures*. Springer; 2019. p.345-358.